THE APPLICATION OF CHANNELIZED HOTELLING OBSERVER IN LESION DETECTION IN HEPATIC SPECT IMAGES

Tawatchai EKJEEN, MSc,[1] Chiraporn TOCHAROENCHAI, PhD,[1] Pawana PUSUWAN, MD[2]

OBJECTIVE: The purposes of the study were to apply the channelized hotelling observer (CHO) to study factors affecting lesion detectability in hepatic single photon emission computed tomography (SPECT) images.

MATERIALS AND METHODS: The 4-dimensional NURBS-based Cardiac-Torso (4D NCAT) phantom was used with organ uptake ratios related to the biodistribution of ^{99m}Tc-hydrazinonicotinyl-Tyr^{3}-octreotide (^{99m}Tc-HYNIC-TOC) at 4 hrs after injection. The Monte Carlo simulation, simulation system for emission tomography (SIMSET) code, was used to generate projection data of 128x128 matrix size and 120 views over 360 degrees. To study factors affecting lesion detectability, 3 different sizes of 8-mm, 10-mm and 15-mm with a lesion contrast ratio of 2:1 were created with count density of ~5 M counts. To study the detectability of 8-mm lesion size, the lesion contrast ratios of 2:1 and 5:1 were investigated and 2 different count densities of ~5 M and ~10 M counts at lesion contrast ratio of 2:1 were also studied. Ninety projection data of lesion-present and lesion-absent for each test condition were generated for CHO application. To reconstruct images, ordered subset expectation maximization (OSEM) algorithm with 2 iterations and 4 subsets were used with Butterworth filter at cutoff frequency of 0.25 cycle/pixel and order of 10. The area under curve (AUC) was used as lesion detectability index.

RESULTS: The results showed that at lesion contrast ratio of 2:1 with ~5 M counts, the AUCs of 8-mm, 10-mm and 15-mm lesion sizes were 0.6119, 0.7176 and 0.9795, respectively, and the AUC of 8-mm lesion with lesion contrast ratio of 5:1 was 0.9308. At count densities of ~5 M and ~10 M counts, the AUCs were 0.6119 and 0.7160, respectively.

CONCLUSION: In conclusion, the detectability was increased with lesion size and lesion contrast ratio. However, this study showed that the detectability was slightly increased when increasing the count density. It may be due to the limitation of the performance characteristics of the imaging system. Moreover, this study demonstrated that CHO is a good research tool for lesion detectability.

Keywords: Channelized Hotelling Observer, Lesion detection, Monte Carlo simulation, NCAT phantom

1 Department of Radiological Technology, Faculty of Medical Technology, Mahidol University
2 Division of Nuclear Medicine, Department of Radiology, Siriraj Hospital

Recently, a Tc-99m-labeled somatostatin analog based on Tyr^{3}-octreotide (TOC) and hydrazinonicotinic acid (HYNIC) has been developed. This radiopharmaceutical has a similar biodistribution to In-111-diethylenediaminepentaacetic acid-D-Phe^{1}-octreotide (^{111}In-DTPA-octreotide), rapid tumor uptake, on-site availability and low costs.[1,2] For lesion detection using ^{99m}Tc-HYNIC-TOC, Gabriel et al[1] found the 3 small metastases in the right liver lobe and 2 small metastases in the left liver lobe, all of which were in the range of 1.0 cm. Moreover, a solitary pulmonary metastasis of a papillary carcinoma of the thyroid gland was found and a lesion size of this metastasis was 1.3x1.4 cm. Bangard et al[3] found a medullary thyroid carcinoma with a diameter of 7 mm located in the posterior basal lobe of the left lung. Dydejczyk et al[4] found a smallest lesion size of 4 mm in the patient of rectal tumor. Several studies mentioned that detection of liver metastasis by somatostatin analogues was very important. Because the liver represents the most commonly site of metastases in neuroendocrine tumors and the survival rate of patient with liver involvement was decreased when compared with nonmetastases liver disease.[5,6] Thus the liver was an organ of interest for the lesion detectability in ^{99m}Tc-HYNIC-TOC single photon emission computed tomography (SPECT) images.

A preliminary study of ^{99m}Tc-HYNIC-TOC SPECT imaging has recently been performed at Division of Nuclear medicine, Department of Radiology, Faculty of Medicine, Siriraj Hospital. The lesions in the liver less than 15 mm in diameter were difficult to detect. Human observer study has been widely used for medical image quality assessment. Due to many drawbacks of human observer study, the channelized hotelling observer (CHO), a linear observer, was of interest. Several studies[7,8] found that CHO provided good predictions with the results of human observer study. The aim of this study was to study factors affecting on lesion detectability such as lesion size, lesion contrast ratio and count density in hepatic SPECT.

MATERIALS AND METHODS

Phantom Design

The 4-dimensional NURBs-based Cardio-Torso (NCAT) phantom was used to provide a realistic model of the activity distribution of ^{99m}Tc-HYNIC-TOC at 4 hrs after injection. The organ uptake ratios in NCAT phantom were obtained from five patients at Division of Nuclear medicine, Department of Radiology, Siriraj Hospital. To study of the effect of lesion size on lesion detectability, three different sizes of 8-mm, 10-mm and 15-mm were generated with lesion contrast ratio of 2:1. This lesion contrast ratio was obtained from patients who underwent ^{99m}Tc-HYNIC-TOC SPECT imaging at Division of Nuclear Medicine, Siriraj Hospital. Moreover, factors affecting lesion detectability of a small lesion of 8-mm was interested. The effects of lesion contrast ratio and count density on lesion detectability were studied. For the effect of lesion contrast ratio on lesion detectability, two different lesion contrast ratios of 2:1 and 5:1 (from Meisetschlager et al[9] were selected. To study the effect of count density on lesion detectability of the 8-mm lesion size with lesion contrast ratio of 2:1, two count densities of ~5 M counts (~10 mCi) and ~10 M counts (~20 mCi) were used. The count density of ~5 M counts was obtained from the count density of the patients who was injected of ~10 mCi and assuming that the count density of ~10 M counts would obtain from the injection of ~20 mCi ^{99m}Tc-HYNIC-TOC. For each study, three different locations of lesion in the liver were set as shown in Figure 1. In summary, there were 4 sets of phantom for lesion-present and 1 phantom for lesion-absent used in this study (Figure 1).

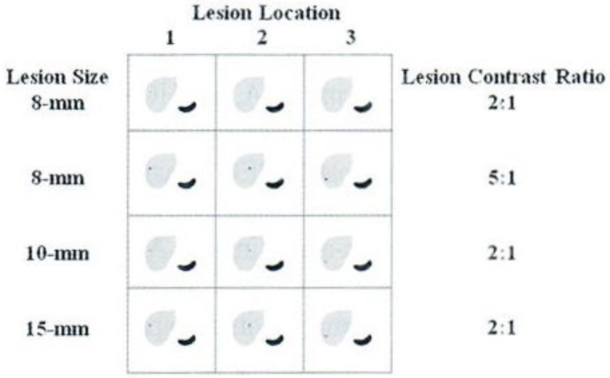

Fig.1 Four sets of phantom with different lesion sizes and different lesion contrast ratios; 8-mm with lesion contrast ratio of 2:1 (first row), 8-mm with lesion contrast ratio of 5:1 (second row). The 10-mm (third row) and 15-mm (fourth row) of lesion contrast ratio of 2:1.

Projection Data Generation and Image Reconstruction

To generate projection data, the Monte Carlo simulation, simulation system for emission tomography (SIMSET) code was used.[10] The clinical protocol used for ^{99m}Tc-HYNIC-TOC SPECT imaging at Division of Nuclear Medicine, Siriraj Hospital was used in the simulation as followed. SPECT system with 3/8 inch of thallium-activated sodium iodide NaI(Tl) crystal was modeled and equipped with low-energy high resolution collimator. Energy window width was set at 20% of 140 keV. The projection data were generated using 128x128 matrix size with bin size of 3.45 mm at 25 cm radius of rotation and 120 views over 360 degrees. For the study of the effects of lesion size and lesion contrast ratio on lesion detectability, the projection data were generated at count density of ~5 M counts. For the effect of count density on lesion detectability, the projection data were generated at two different count densities of ~5 M counts and ~10 M counts. To be used in CHO study, an equal number of lesion-present and lesion-absent projection data were used. To obtain 90 lesion-present images (30 images for training and 60 images for testing) for each test condition, 30 projection data with different noise realizations were generated for each phantom (3 different locations of the lesion). To obtain 90 lesion-absent images, 90 projection data with different noise realizations were created. Each projection data was reconstructed using iterative ordered subset expectation maximization (OSEM) algorithm with 4 subsets and 2 iterations (a clinical protocol). To smooth the image noise, Butterworth filter with order of 10 at cutoff frequency of 0.25 cycle/pixel was used. The reconstructed images with matrix size of 128x128 for the effects of lesion size, lesion contrast ratio and count density on lesion detectability studies are shown in Figure 2-4, respectively. To run CHO study, the image slice which was at the center of the lesion was selected and extracted into 32x32 matrix size which the lesion was in the field of view with random locations.

Application of Channelized Hotelling Observer

Traditionally, a task-based evaluation for a defect detection task has required human observer study. However, this observer is time consuming. To recruit physicians to perform observer study is also difficult. From the drawbacks of human observer, the channelized hotelling observer was used.

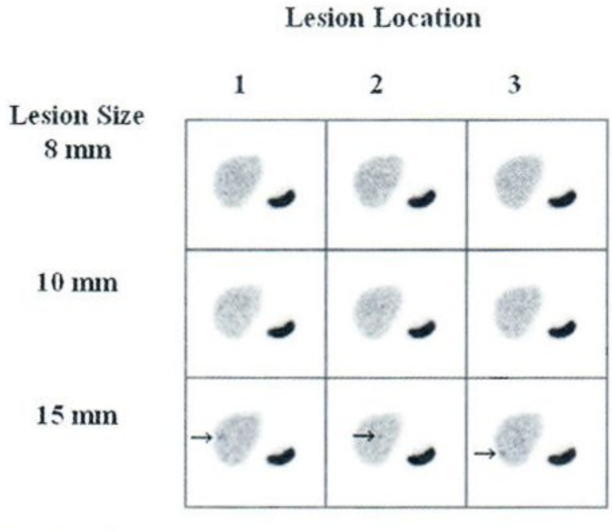

Fig.2 Reconstructed images of 3 sets of phantom with different lesion sizes; 8-mm (top row), 10-mm (middle row) and 15-mm (bottom row) of lesion contrast ratio of 2:1, at count density of ~5 M counts.

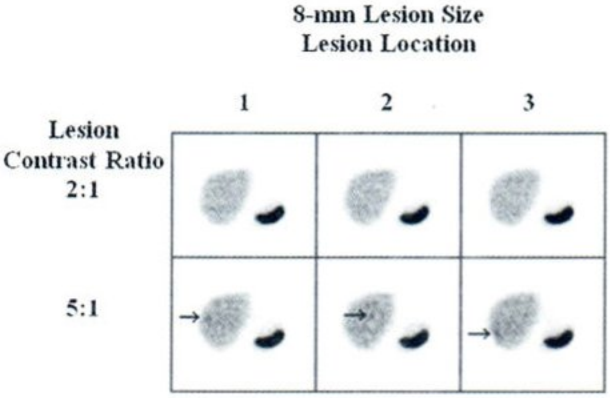

Fig.3 Reconstructed images of 2 sets of phantom of 8-mm lesion size with 2 different lesion contrast ratios; 2:1 (top row) and 5:1 (bottom row), at count density of ~5 M counts.

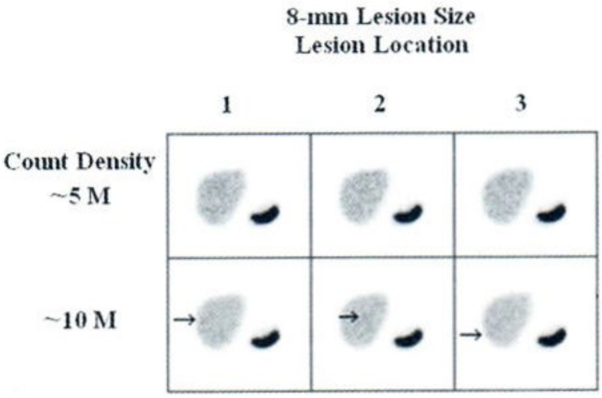

Fig.4 Reconstructed images of 2 sets of phantom of 8-mm lesion size of lesion contrast ratio of 2:1 with 2 different count densities; ~5 M counts (top row) and ~10 M counts (bottom row).

The CHO software program used in this study was contributed from Professor Eric C. Frey, Johns Hopkins University, USA. In CHO study, there were two classes of image including lesion-present and lesion-absent of hepatic SPECT images, resulting in two classes of feature vector corresponding to lesion-present and lesion-absent images. A four-element feature vector of each image was created by taking the dot product of the image with the spatial domain template for each channel. The spatial domain template for each channel was obtained from the frequency domain channel by taking the inverse Fourier Transform following a phase shift to move the center of the template to lesion.[11] Thus there were four frequency domain channels, resulting in four spatial domain channels for three lesion locations as shown in Figure 5.

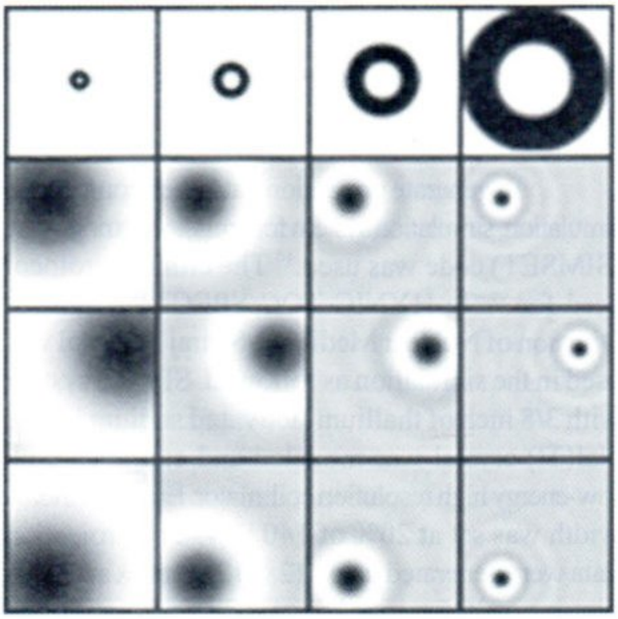

Fig.5 Images with 32x32 matrix size of four frequency-domain channels (first row) and shifted spatial domain templates (second to fourth rows) for three lesion locations.

In this study, the CHO was trained using 30 feature vectors of each class to learn the differences between the two classes of images. After training CHO, the mean vectors and covariance were generated and used later in testing CHO. Once the CHO was trained, it was tested by applying to a different, independent ensemble of feature vectors of each class. Then the CHO was tested using 60 feature vectors of each class. In testing CHO, the mean vectors and covariance were used to formulate a new vector called CHO template vector. After a CHO template vector was then applied to each testing input feature vector by taking the dot product and the scalar value known as the test statistic results.

Receiver Operating Characteristic(ROC) Analysis

The resulting test statistic is analogous to the rating which obtains from a human observer. Thus, the resulting rating data for each test condition were then analyzed using LABROC4 program.[12] This program sorts ranking values and converts to pairs of true positive fraction (TPF) and false positive fraction (FPF) and corresponding area under the curve (AUC) was also given. Finally, the pairs of TPF and FPF used to form the ROC curve and the AUC was used as a lesion detectability index.

RESULTS

The AUC in lesion detection for factors affecting on lesion detectability in hepatic SPECT images such as lesion size, lesion contrast ratio and count density were reported in Table 1. For the effect of lesion size on lesion detectability with lesion contrast-ratio of 2:1, the AUCs of 8-mm, 10-mm and 15-mm lesions were 0.6119, 0.7176 and 0.9795, respectively. The ROC curves of three different lesion sizes were shown in Figure 6. All three curves did not cross each other. It implied that detectability of 15-mm lesion size was better than the other two lesion sizes at all possible confidence thresholds. To study the effect of lesion contrast ratio on the detectability of 8-mm lesion at count density of ~5 M counts, the AUCs of lesion contrast ratio of 2:1 and 5:1 were 0.6119 and 0.9308, respectively. As shown in Figure 7, the ROC curve of lesion contrast ratio of 5:1 was higher than lesion contrast ratio of 2:1 at all possible confidence threshold. To study the effect of count density on the detectability of 8-mm lesion at lesion contrast ratio of 2:1, the AUCs of count density of ~5 M counts and ~10 M counts were 0.6119 and 0.7160, respectively. The ROC curves of two different count densities were shown in Figure 8. The plot showed that the curves did not cross each other implying that the detectability of count density of ~10 M counts was better than the count density of ~5 M counts at all possible confidence thresholds.

Table 1 The AUC in lesion detection for factors affecting lesion detectability in hepatic SPECT images such as lesion size, lesion contrast ratio and count density.

Lesion Size (mm)	Lesion Contrast Ratio	Count Density	AUC
8	2:1	~5 M	0.6119
8	2:1	~10 M	0.7160
8	5:1	~5 M	0.9308
10	2:1	~5 M	0.7176
15	2:1	~5 M	0.9795

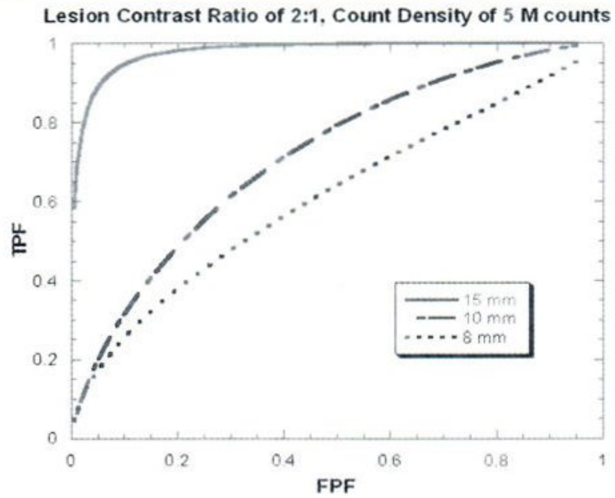

Fig.6 The ROC curves of three different lesions; 8-mm, 10-mm and 15-mm with lesion contrast ratio of 2:1 for projection data of ~5 M counts.

DISCUSSION

In this study, the application of CHO results of this study showed that the 15-mm lesion was clearly seen, the detectability of 10-mm lesion was fair and the 8-mm lesion was difficult to be detected with lesion contrast of 2:1 at count density of ~5 M counts. The results agreed with Dromain et al.[6] They found that the trend of the detection of liver metastases was better when the lesion size was more than 15 mm. Similarly, Gabriel et al[1] found that all of lesion sizes that were seen in the liver were in the range of 10 mm.

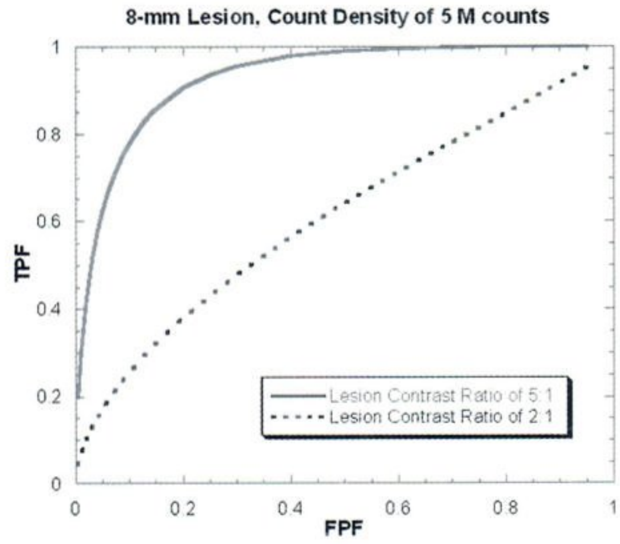

Fig.7 The ROC curves of two different lesion contrast ratios; 2:1 and 5:1 of 8-mm lesion for projection data of ~5 M counts.

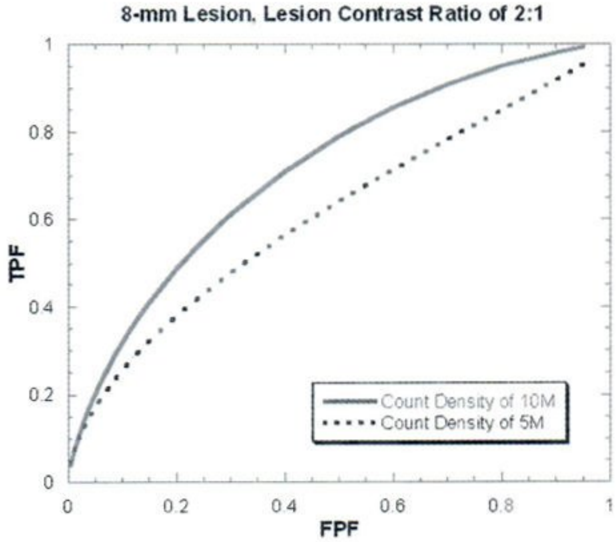

Fig.8 The ROC curves of ~5 M counts and ~10 M counts of 8-mm lesion with lesion contrast ratio of 2:1.

For the effect of lesion contrast ratio on lesion detectability, the detectability of 8-mm lesion was improved when the lesion contrast ratio was increased from 2:1 to 5:1. This result agreed with Meisetschlager et al.[9] They investigated the tumor contrast ratios in the liver and the result revealed that the mean tumor contrast ratio was approximately to 5:1. Moreover, this study showed that the lesion detectability of 8-mm lesion with count density of ~5 M counts was poor, the lesion detectability was slightly better when increasing the number of count density to ~10 M counts. The detectability may be borderlined for this SPECT system, regarding the range of 5.6 mm to 11.1 mm of the system resolution. That means the 8-mm lesion detectability can be seen with noise -free data. In clinical situation, to increase count density can be achieved by increasing either injection dose or scanning time or both. Good patient cooperation should be aware.

Another aspect of this study was to demonstrate the application of CHO for lesion detectability. Although, CHO needs a large number of images, computational time is short and repetition of the experiment is easily to perform. Furthermore, it is very useful tool for a preliminary study.

Therefore, CHO is a good research tool for lesion detectability.

Limitations of This Research

The data used in this study were simulated based on clinical studies. However, there were several limitations in this study. Firstly, the effects of attenuation, collimator-detector response and scatter were not modeled. Secondly, the variation of lesion locations was not sufficient (3 locations), it may affect the results in terms of over-estimated AUC. Thirdly, CHO provides only the relative AUC and human observers give absolute AUC. For these reasons, the results of this study can be served as guidelines in the clinical situation. Although, CHO becomes the good research tool for lesion detectability, the human observer study is still needed for the reliable and acceptable method to evaluate the image quality and the performance of diagnostic test.

ACKNOWLEDGEMENTS

The authors would like to thank Professors Benjamin M.W. Tsui and Eric C. Frey, Dr. Xin He and Dr. William Paul Segars, Department of Radiology, Johns Hopkins University, USA for CHO software program, phantom and the valuable advices. The authors also thank to the University of Washington, USA for SIMSET software program and the staffs at Division of Nuclear Medicine, Department of Radiology, Siriraj Hospital for their help in the preliminary study of ^{99m}Tc-HYNIC-TOC imaging.

REFERENCES

1. Gabriel M, Decristoforo C, Donnemiller E, Ulmer H, Rychlinski CW, Mather SJ, et al. An intrapatient comparison of ^{99m}Tc-EDDA/HYNIC-TOC with 111In-DTPA-Octretide for diagnostic of somatostatin receptor -expressing tomors. J Nucl Med 2003; 44: 708-16.
2. Decristoforo C, Mather SJ, Cholewinski W, Donnemiller E, Riccabona G, Moncayo R. ^{99m}Tc-EDDA/HYNIC-TOC: a new ^{99m}Tc -labelled radiopharmaceutical for imaging somatostatin receptor-positive tomours: first clinical results and intra-patient comparison with ^{111}In-labelled octreotide derivatives. Eur J Nucl Med 2000; 27: 1318-25.
3. Bangard M, Béhé M, Guhlke S, Otte R, Bender H, Maecke HR, et al. Detection of somatostatin receptor-positive tumors using the new ^{99m}Tc-tricine-HYNIC-D-Phe-Try^3-octreotide: first results in patients and comparison with ^{111}In-DTPA-D-Phe-octretide. Eur J Nucl Med 2000; 27: 628-37.
4. Dydejczyk AH, Baron KF, Mikolajczak R, Maecke HR, Huszno B, Pach D, et al. ^{99m}Tc-EDDA/HYNIC-octreotate scintigraphy, an efficient method for the detection and staging of carcinoid tumours: results of 3 years' experience. Eur J Nucl Med Mol Imaging 2006; 33: 1123-33.
5. Schillaci O, Spanu A, Scopinaro F, Falchi A, Danieli R, Marongiu P, et al. Somatostatin receptor scintigraphy in liver metastasis detection from gastroenteropancreatic neuroendocrine tumors. J Nucl Med 2003; 44: 359-68.
6. Dromain C, de Baere T, Lumbroso J, Caillet H, Laplanche A, Boige V, et al. Detection of liver metastases from endocrine tumors: a prospective comparison of somatostatin receptor scintigraphy, computed tomography, and magentic resonance imaging. J Clin Oncol 2005; 23: 70-8.
7. Gifford HC, King MA, de Vries DJ, Soares EJ. Channelized Hotelling and human observer correlation for lesion detection in hepatic SPECT imaging. J Nucl Med 2000; 41: 514-21.
8. Smith WE, Barrett HH. Hotelling trace criterion as a figure of merit for the optimization of imaging systems. Opt Soc Am 1986; 3: 717-25.

9. Meisetschlager G, Poethko T, Stahl A, Wolf I, Scheidhauer K, Schottelius M, et al. Gluc-Lys ([^{18}F]FP)-TOCA PET in patients with SSTR-positive tumors: biodistribution and diagnostic evaluation compared with [^{111}In] DTPA-octreotide. J Nucl Med 2006; 47: 566-73.
10. SimSET homepage [Homepage on the internet]. USA: Washington University; [cite 2008 Mar 20]. Available from: URL: http://depts.washington.edu/~simset/html/simset_main.html.
11. Frey EC, Gilland KL, Tsui BMW. Application of task-based measures of image quality to optimization and evaluation of three-dimensional reconstruction-based compensation methods in myocardial perfusion SPECT. IEEE Trans Med Imag 2002; 20: 1040-50.
12. Metz CE, Herman BA, Shen JH. Maximum likelihood estimation of receiver operating characteristic (ROC) curves from continuously -distributed data. Statist Med 1998; 17: 1033-53.